AIP | Journal of Applied Physics

Large magnetic entropy and electron-phonon coupling in Gd-based metallic glass

M. B. Tang, L. Xia, K. C. Chan, and J. T. Zhao

Citation: J. Appl. Phys. **112**, 113503 (2012); doi: 10.1063/1.4768263
View online: http://dx.doi.org/10.1063/1.4768263
View Table of Contents: http://jap.aip.org/resource/1/JAPIAU/v112/i11
Published by the AIP Publishing LLC.

Large magnetic entropy and electron-phonon coupling in Gd-based metallic glass

M. B. Tang,[1,a)] L. Xia,[2] K. C. Chan,[3] and J. T. Zhao[1]
[1]*Key Laboratory of Transparent and Opto-functional Inorganic Materials, Shanghai Institute of Ceramics, Chinese Academy of Sciences, Shanghai 200050, China*
[2]*Institute of Materials, Shanghai University, Shanghai 200072, China*
[3]*Department of Industrial and Systems Engineering, The Hong Kong Polytechnic University, Hung Hom, Kowloon, Hong Kong*

(Received 15 August 2012; accepted 1 November 2012; published online 4 December 2012)

We study the magnetic entropy behavior in $Gd_{55}Al_{20}Ni_{12}Co_{10}Mn_3$ metallic glass by magnetic susceptibility, resistivity, and specific heat at low temperatures. The Gd-based metallic glass shows metallic behavior, and a ferromagnetic to paramagnetic transition at 106 K. The ferromagnetic order assists the electron-phonon coupling, which induces the large excess magnetic entropy below Curie temperature in the Gd-based metallic glass. The results are important to understand the electron-phonon coupling behavior in disordered alloys. © *2012 American Institute of Physics*. [http://dx.doi.org/10.1063/1.4768263]

I. INTRODUCTION

The rare earth based bulk metallic glasses (BMGs) show unusual physical properties and potential applications as functional materials, and have attracted considerable attention.[1] Since the rare earth Nd-based BMGs were found in 1996, a series of Ce-, Pr-, Sm-, Gd-, Tb-, Dy-, Ho-, Er-, Yb-, and Tm-based rare earth BMGs have been developed.[1] In the rare earth based BMGs, the rare earth elements have the magnetic 4*f* electrons, which shows plentiful physical properties, for example, magnetic properties,[2] elastic behavior,[3] and heavy fermion behavior, etc.[4] The rare earth based BMGs with disordered structure exhibit a high effective moment and excellent magnetocaloric effect in magnetic field. Therefore, the rare earth based BMGs have attracted intense interests as magnetic refrigeration materials recently.[5–8] In contrast to crystalline compounds, the disordered BMGs have a broadened magnetic entropy change peak and high value of refrigerant capacity. The properties of metallic glasses can be also modulated by annealing and the composition.[1,7] These features drew the attention of researchers searching for systems with promising magnetocaloric properties.

Except for the magnetocaloric effect in magnetic field, the magnetic moment-electron or the electron-phonon interaction in zero magnetic field in the disordered structure may exists.[9,10] This has been illustrated in Ce-based BMG and GdSi amorphous alloys.[11–13] Ce-based BMGs with excellent glass-forming ability have been extensively studied.[11] One of the important properties is the anomalous softening acoustic behavior, which is only observed in Ce-based amorphous alloys.[12] Recently, the studies on specific heat reveals that the Ce-based BMG has large excess entropy in zero magnetic field at low temperatures. The excess entropy in the Ce-based BMG includes the contributions of both magnetic entropy of Ce^{3+} ion and strong electron-phonon coupling,[10] which is induced by the valence instability. The GdSi amorphous alloy undergoes a metal-insulator transiotion.[13] Near the transition, the moment-electron interaction enhances the localization of the conduction electrons, and causes negative magnetoresistance. The localized electron mainly persists into the insulating side of the transition, and exhibits large excess entropy which is confirmed by specific heat studies.[9] At present, the large excess magnetic entropy in the disordered structure is only found in the Ce-based BMG and GdSi amorphous alloy, and is not yet well studied and understood.

The $Gd_{55}Al_{20}Ni_{12}Co_{10}Mn_3$ BMG exhibits a high glass forming ability and excellent magnetocaloric effect.[14] The peak value of the magnetic entropy change is about 8 J kg^{-1} K^{-1}, and the refrigerant capacity value is about 880 J kg^{-1} under the field of 5 T. The value of refrigerant capacity is about 35% higher than that of other alloys reported previously. In this paper, the temperature-dependent magnetization, resistivity, and specific heat C_p of the $Gd_{55}Al_{20}Ni_{12}Co_{10}Mn_3$ BMG is studied, by comparing with that of the isostructural nonmagnetic reference $Y_{55}Al_{20}Ni_{12}Co_{10}Mn_3$ BMG. The results indicate that the Gd-based BMG shows metallic behavior and large excess entropy. The ferromagnetic order assists the electron-phonon coupling below Curie temperature in the Gd-based BMG, which induces the large excess entropy.

II. EXPERIMENTAL DETAILS

The $Gd_{55}Al_{20}Ni_{12}Co_{10}Mn_3$ and $Y_{55}Al_{20}Ni_{12}Co_{10}Mn_3$ BMGs were prepared melting 99.9% (at. %) pure Gd, Y, Al, Ni, Co, and Mn in an arc-melting furnace under argon atmosphere. The glassy structure of the BMGs is ascertained by X-ray diffraction (XRD) using a MAC M03 XHF diffractometer with Cu K_α radiation, and differential scanning calorimeter (DSC). DSC measurement was carried out in a Perkin-Elmer DIAMOND DSC at a heating rate of 20 K/min. The low temperature properties of the heat capacity, magnetization, and resistivity were measured using physical property measurement

a)Author to whom correspondence should be addressed. Electronic mail: mbtang@mail.sic.ac.cn.

system (PPMS, Quantum Design Inc.) from 2 K to 300 K. The magnetic susceptibility was measured after zero-field-cooling (ZFC) and field-cooling (FC).

III. RESULTS AND DISCUSSIONS

A. Glassy structure

The glassy structure of the BMGs is determined by XRD and DSC. The XRD patterns of the $Gd_{55}Al_{20}Ni_{12}Co_{10}Mn_3$ and $Y_{55}Al_{20}Ni_{12}Co_{10}Mn_3$ BMGs (not shown) indicate that the samples exhibit a broad diffraction maxima characteristic of metallic glasses. The DSC traces were obtained at heating rate of 20 K/min, which is shown in Fig. 1. The obvious endothermic characteristic before crystallization demonstrates a distinct glass transition. Following the glass transition, the obvious exothermic heat release events are observed, which are associated with the transformations from the undercooled liquid state to the equilibrium crystalline state. The distinct glass transition and the sharp crystallization event further confirms the glassy nature of BMGs.

B. Magnetic susceptibility

The *dc* magnetic susceptibility of the $Y_{55}Al_{20}Ni_{12}Co_{10}Mn_3$ BMG was measured at $H = 500$ Oe after ZFC (Figure 2), and is very weak, which confirms that the reference $Y_{55}Al_{20}Ni_{12}Co_{10}Mn_3$ BMG is nonmagnetic. The magnetic susceptibility of the $Gd_{55}Al_{20}Ni_{12}Co_{10}Mn_3$ BMG was measured at $H = 200$ Oe after ZFC and FC (see Fig. 2). The magnetic transition temperature of the $Gd_{55}Al_{20}Ni_{12}Co_{10}Mn_3$ BMG is about 106 K. Below the transition temperature, the ZFC and FC susceptibility is no obviously different, which confirms that there is no spin glass-type transition for the Gd-based BMG, and the magnetic phase transition is due to ferromagnetic to paramagnetic transition with the Curie temperature 106 K.

C. Heat capacity

The specific heat C_p of the $Gd_{55}Al_{20}Ni_{12}Co_{10}Mn_3$ and $Y_{55}Al_{20}Ni_{12}Co_{10}Mn_3$ BMGs is measured from 2 K to 300 K (as shown in Fig. 3). The specific heat of the Gd-based BMG is larger than that of the Y-based BMG in the temperature range from 2 K to 300 K, and shows a peak near 101 K which is consistent with the magnetic results. With the temperature increase, the specific heat C_p (molar-atom) gradually reaches a constant value (26.5 mol^{-1} K^{-1} and 25.7 mol^{-1} K^{-1} at 303 K for the $Gd_{55}Al_{20}Ni_{12}Co_{10}Mn_3$ and $Y_{55}Al_{20}Ni_{12}Co_{10}Mn_3$ BMGs, respectively), which is close to the classical Dulong-Petit value 24.9 $J{\cdot}mol^{-1}$ K^{-1}. The C_p/T vs. T^2 is plotted in the temperature range from 2 K to 14.9 K, (the inset in Fig. 3). In the temperature range $66 < T^2 < 222$ K^2, the data of the Y-based BMG are well fitted in a polynomial form $C_p/T = \gamma + \beta T^2$ with $\gamma = 10.56$ $mJ{\cdot}mol^{-1}$ K^{-2} and

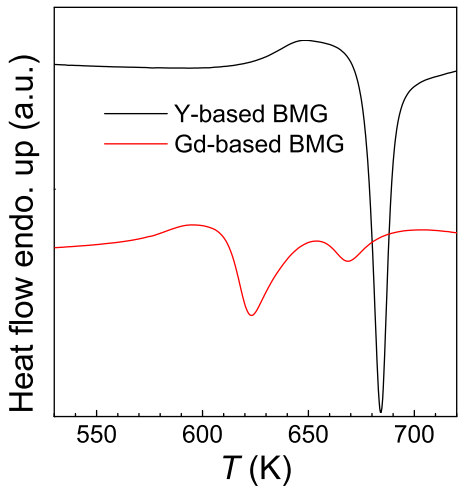

FIG. 1. DSC traces of the alloys showing the glass transition and crystallization process. The scanning rate is 20 K/min.

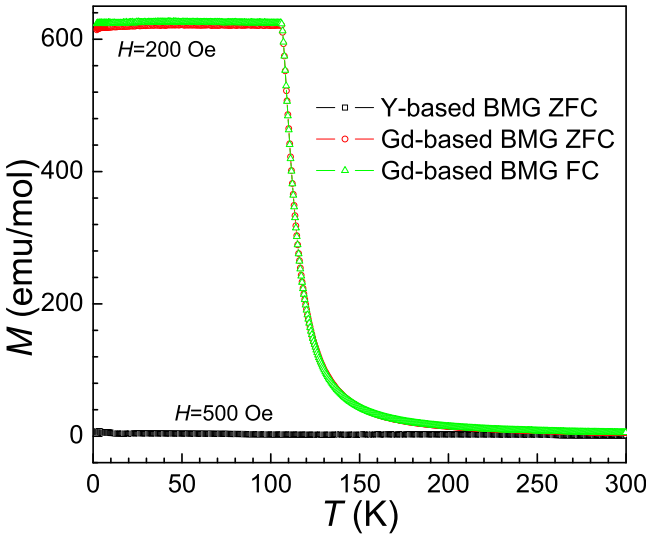

FIG. 2. *dc* magnetic susceptibility M vs. T for the $Gd_{55}Al_{20}Ni_{12}Co_{10}Mn_3$ and $Y_{55}Al_{20}Ni_{12}Co_{10}Mn_3$ BMGs.

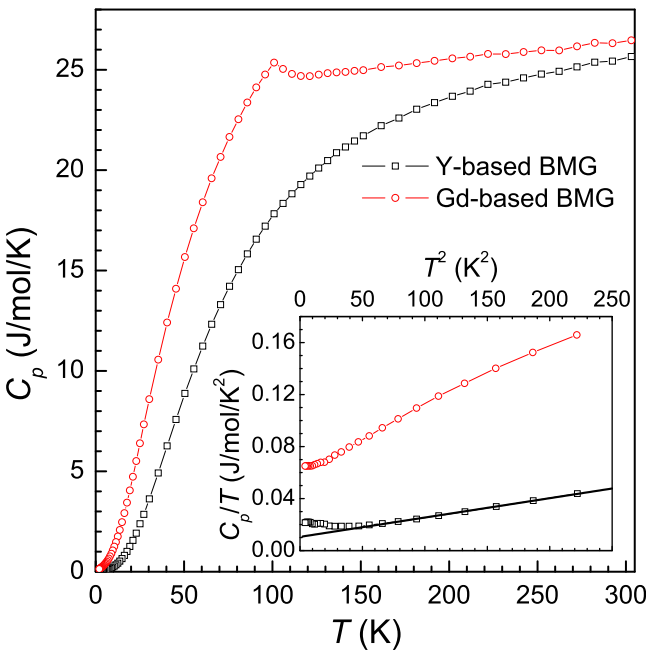

FIG. 3. Specific heat C_p of the $Gd_{55}Al_{20}Ni_{12}Co_{10}Mn_3$ and $Y_{55}Al_{20}Ni_{12}Co_{10}Mn_3$ BMGs in the temperature range from 2 K to 300 K. Inset: Specific heat, shown as C_p/T vs. T^2 at low temperature, the solid line is the fitting result of the specific heat between 8.1 K and 14.9 K using the expression: $C_p/T = \gamma + \beta T^2$ for the $Y_{55}Al_{20}Ni_{12}Co_{10}Mn_3$ BMG.

$\beta = 148.7\ \mu J \cdot mol^{-1}\ K^{-4}$. The θ_D is derived to be 236 K by $\beta = \frac{12\pi^4 R}{5}\frac{1}{\theta_D^3}$ (where R is the gas constant). Just like other BMGs,[15] in the lower temperature range, the data of the Y-based BMG are deviated from the linear behavior. The deviation in the BMGs could be ascribed to the tunneling state effect.[15] Due to the ferromagnetic effect at low temperature, the C_p/T vs. T^2 plot of the $Gd_{55}Al_{20}Ni_{12}Co_{10}Mn_3$ BMG is larger than that of the $Y_{55}Al_{20}Ni_{12}Co_{10}Mn_3$ BMG, and deviated from the linear behavior.

D. Excess specific heat and entropy

The excess specific heat ΔC_p of the $Gd_{55}Al_{20}Ni_{12}Co_{10}Mn_3$ is obtained by subtracting the C_p of the $Y_{55}Al_{20}Ni_{12}Co_{10}Mn_3$ glass [Fig. 4(a)]. The excess specific heat ΔC_p of the $Gd_{55}Al_{20}Ni_{12}Co_{10}Mn_3$ increases rapidly with decreasing temperature from room temperature, and shows a peak near 101 K and an obvious hump below the peak. The simple extrapolation in the glasses is made by drawing straight lines from the lowest temperature data point to $T = 0$, $\Delta C_p = 0$. The entropy of the excess specific heat for the $Gd_{55}Al_{20}Ni_{12}Co_{10}Mn_3$ BMG can be got by $S = \int_{T_{min}}^{T_{max}} \frac{\Delta C_p}{T} dT$, and is exhibited in Fig. 4(b). The value of S is about 26.9 J/mol-Gd/K at 303 K. The total magnetic entropy of Gd^{3+} ion ($s_{Gd} = 7/2$) is $S = R\ln(2s_{Gd} + 1) = 17.3$ J/mol-Gd/K, here R is the gas constant. Like that of the $Ce_{68}Al_{10}Cu_{20}Co_2$ BMG,[10] S for the $Gd_{55}Al_{20}Ni_{12}Co_{10}Mn_3$ BMG is thus comparable to or exceeds the total available from gadolinium moments. Data below the peak would contribute to significantly more entropy, and the large total S suggests that there is the contribution of strong electron-phonon coupling,[10] or the localized electron moments in the Gd-based BMG.[9]

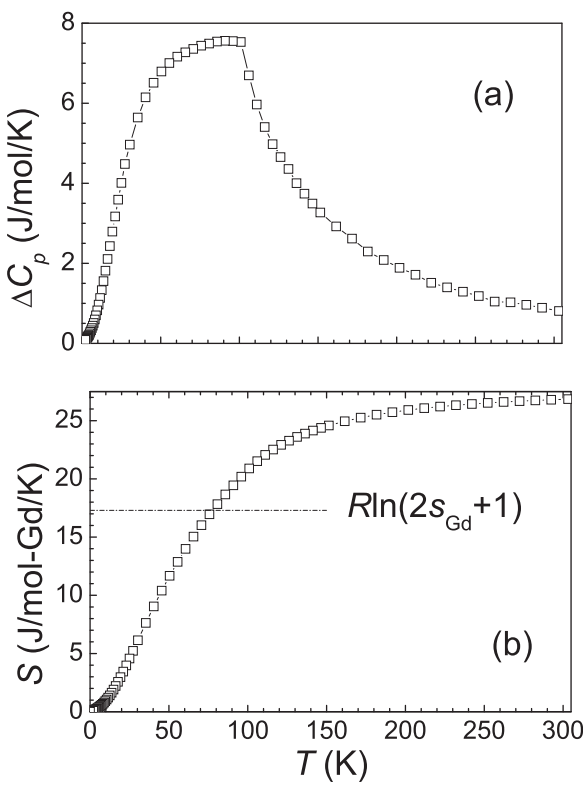

FIG. 4. Excess specific heat ΔC_p (a) and entropy ΔS (b) of the $Gd_{55}Al_{20}Ni_{12}Co_{10}Mn_3$ BMG.

E. Resistivity

To further study the large total magnetic entropy in the Gd-based BMG, the electrical resistivity of both $Gd_{55}Al_{20}Ni_{12}Co_{10}Mn_3$ and $Y_{55}Al_{20}Ni_{12}Co_{10}Mn_3$ BMGs in the low temperature range was measured and is exhibited in Fig. 5(a) (normalized at 2 K). By the resistivity results, both BMGs exhibit a metallic behavior in the measured temperature range, and the change of the resistivity of both BMGs in the measured temperature range is very small, and less than 4%. Due to the tunneling state effect, the resistivity of both BMGs below about 20 K increases with decreasing temperature.[16] Above 20 K, the temperature coefficient of the resistivity is different, positive for the $Y_{55}Al_{20}Ni_{12}Co_{10}Mn_3$ BMG and negative for the $Gd_{55}Al_{20}Ni_{12}Co_{10}Mn_3$ BMG, respectively. Like the specific heat, the resistivity of the $Gd_{55}Al_{20}Ni_{12}Co_{10}Mn_3$ BMG shows an obvious hump near 100 K, which is due to the magnetic phase transition.

The strong localization behavior of the electron in disordered structure has been studied,[17–19] which can induce a metal-insulator transition and a positive magnetoresistivity effect in amorphous materials. Moreover, the $Gd_{55}Al_{20}Ni_{12}Co_{10}Mn_3$ BMG is metallic in the measured temperature range. On the other hand, the magnetoresistivity of the $Gd_{55}Al_{20}Ni_{12}Co_{10}Mn_3$ BMG at 2 K weakly decreases with increasing magnetic field up to 5 T, shown in Fig. 5(b) and normalized at 0 T. The metallic behavior and the negative magnetoresistivity behavior of the Gd-based BMG in the measured temperature range is greatly different from that of GdSi amorphous alloy, which illustrates that the localized

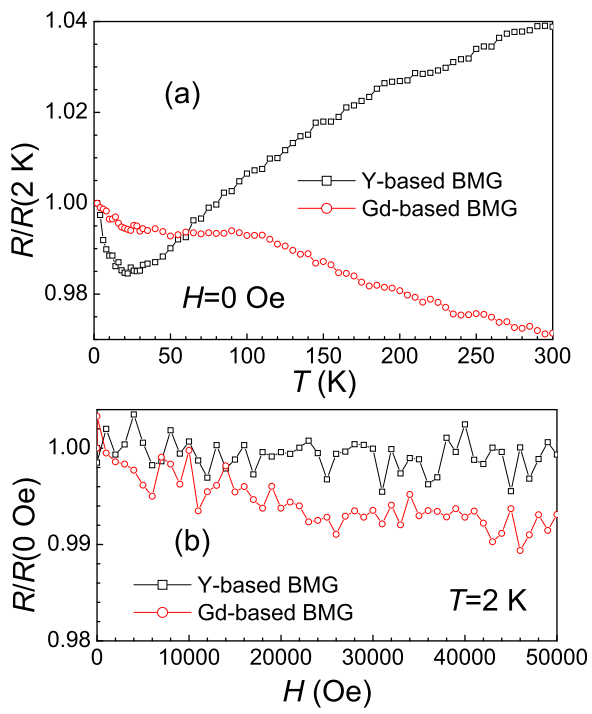

FIG. 5. (a) Electrical resistivity of the $Gd_{55}Al_{20}Ni_{12}Co_{10}Mn_3$ and $Y_{55}Al_{20}Ni_{12}Co_{10}Mn_3$ BMGs above 2 K. (b) Normalized magnetoresistivity of the $Gd_{55}Al_{20}Ni_{12}Co_{10}Mn_3$ and $Y_{55}Al_{20}Ni_{12}Co_{10}Mn_3$ BMGs at 2 K.

effect of the electron is not present and also the localized electron moments may be very weak. The analysis of the resistivity reveals that the large total magnetic entropy in the Gd-based BMG is induced by the strong electron-phonon coupling, not by the localized electron moments.

F. Electron-phonon coupling

In the $Gd_{55}Al_{20}Ni_{12}Co_{10}Mn_3$ BMG, the excess specific heat mainly includes the contributions of both magnetic moment and electron-phonon coupling ($\Delta C_p = C_M + C_{ep}$). It is difficult to determine the electron-phonon coupling contribution or the magnetic contribution. In ferromagnetic compounds, the magnetic specific heat C_M at low temperature usually obeys the T^{α}-law with $\alpha = 1.5$.[20] Fig. 6(a) shows $\ln(\Delta C_p)$ vs. $\ln(T)$ for the $Gd_{55}Al_{20}Ni_{12}Co_{10}Mn_3$ BMG. Like most ferromagnetic compounds, ΔC_p of the ferromagnetic $Gd_{55}Al_{20}Ni_{12}Co_{10}Mn_3$ BMG follows the T^{α}-law with $\alpha = 1.12$ in the temperature range from 2 K to 4 K, which is shown by solid line in Fig. 6(a). The low α value in the Gd-based BMG is maybe due to the effect of the strong disorder structure. At the magnetic phase transition temperature 100 K, the fitted magnetic specific heat value is also close to the total excess specific heat ΔC_p. So we can determine the magnetic specific heat C_M below the phase transition temperature 100 K by the fitted T^{α}-law. Above the phase transition temperature 100 K, the excess specific heat ΔC_p is mainly due to the magnetic specific heat contribution. So the electron-phonon specific heat of the alloy is determined by subtracting the magnetic contribution, ($C_{ep} = \Delta C_p - C_M$), shown in Fig. 6(b). The effect of the electron-phonon coupling is obvious near about 45 K.

The entropy of the magnetic moment S_M and the electron-phonon coupling S_{ep} for the $Gd_{55}Al_{20}Ni_{12}Co_{10}Mn_3$ BMG is obtained by the specific heat of the magnetic moment C_M and electron-phonon coupling C_{ep}, respectively, and is exhibited in Fig. 7. With the temperature increase, the entropy of the magnetic S_M increases rapidly below the magnetic phase transition temperature, and gradually reaches a constant value of 17.0 J/mol-Gd/K at 303 K. The value of S_M at 303 K is close to the total magnetic entropy of Gd^{3+} ion 17.3 J/mol-Gd/K in Fig. 7, which confirms that the analysis of the magnetic specific heat C_M is reasonable. The entropy of the electron-phonon coupling S_{ep} increases gradually above 10 K, and gradually reaches a constant value of 9.9 J/mol-Gd/K at 303 K.

The electron-phonon coupling behavior exists extensively in glass or amorphous materials by both theories and experiments.[10,21–23] Localized states in glassy or amorphous materials exhibit a large electron-phonon coupling by density-functional theory.[21] On the other hand, glasses exist in a nonequilibrium state, and relax toward the metastable equilibrium. The acoustic results of metallic glasses have established that the relaxation associates with the electron-phonon coupling.[22,23] The valence instability in the Ce-based BMG also results in the strong electron-phonon coupling due to the large volume difference between two different valence states.[10] The ferromagnetic order can enhance the electron-phonon coupling below the Curie temperature in the Gd-based BMG. So after subtracting the entropy of the isostructural nonmagnetic BMGs, the large excess magnetic entropy in the rare earth-based BMGs is connected with the magnetic 4*f* electron, and is important to understand the electron-phonon coupling behavior in amorphous alloys.

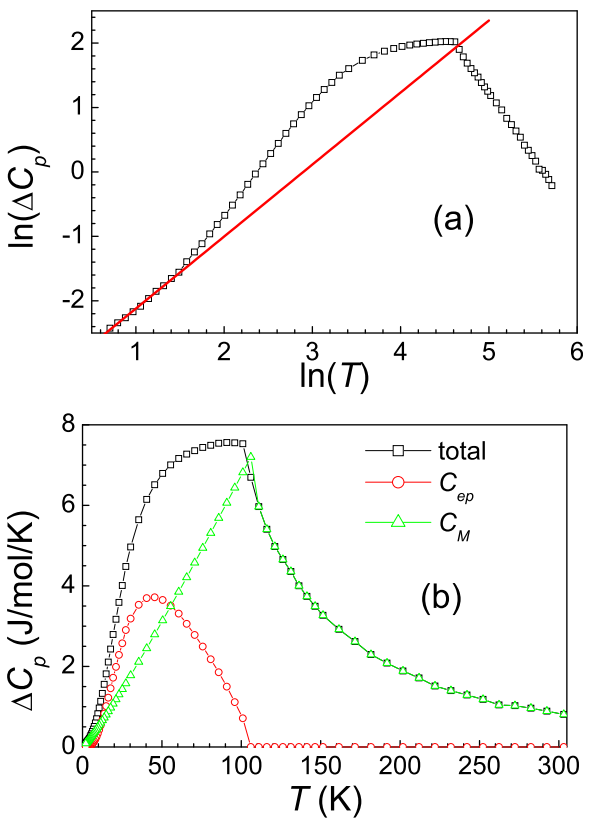

FIG. 6. (a) $\ln(\Delta C_p)$ vs. $\ln(T)$ for the $Gd_{55}Al_{20}Ni_{12}Co_{10}Mn_3$ BMG; the solid line is the linear fitting result below 4 K. (b) Specific heat of magnetic spin and electron-phonon coupling for the $Gd_{55}Al_{20}Ni_{12}Co_{10}Mn_3$ BMG.

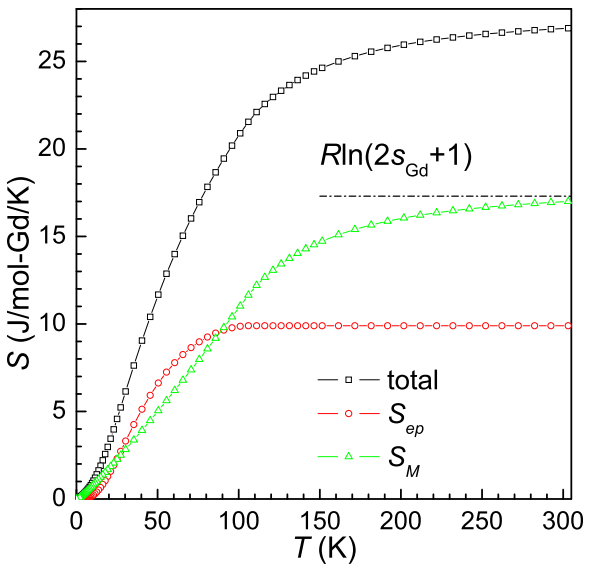

FIG. 7. Entropy of magnetic spin and electron-phonon coupling for the $Gd_{55}Al_{20}Ni_{12}Co_{10}Mn_3$ BMG.

IV. CONCLUSION

The $Gd_{55}Al_{20}Ni_{12}Co_{10}Mn_3$ BMG shows a ferromagnetic to paramagnetic transition at the Curie temperature of 106 K. The specific heat results indicate that there is a large excess magnetic entropy in the Gd-based BMG by comparing with that of the isostructural nonmagnetic $Y_{55}Al_{20}Ni_{12}Co_{10}Mn_3$ BMG. The Gd-based BMG shows metallic behavior by the resistivity results, which illustrates that the localized electron moments are very weak. The ferromagnetic order-assisted electron-phonon coupling below Curie temperature is attributed to the large excess magnetic entropy in the Gd-based metallic glass.

ACKNOWLEDGMENTS

The financial support of the National Science Foundation of China (Grant Nos. 51001113 and 51171100), and the MPG-CAS Partner Group Program is appreciated.

[1]Q. Luo and W. H. Wang, J. Non-Cryst. Solids **355**, 759 (2009).
[2]G. J. Fan, W. Löser, S. Roth, J. Eckert, and L. Schultz, Appl. Phys. Lett. **75**, 2984 (1999).
[3]B. Zhang, R. J. Wang, and W. H. Wang, Phys. Rev. B **72**, 104205 (2005).
[4]M. B. Tang, H. Y. Bai, W. H. Wang, D. Bogdanov, K. Winzer, K. Samwer, and T. Egami, Phys. Rev. B **75**, 172201 (2007).
[5]Q. Luo, D. Q. Zhao, M. X. Pan, and W. H. Wang, Appl. Phys. Lett. **89**, 081914 (2006).
[6]S. Gorsse, B. Chevalier, and G. Orveillon, Appl. Phys. Lett. **92**, 122501 (2008).
[7]Q. Luo and W. H. Wang, J. Alloys Compd. **495**, 209 (2010).
[8]B. Schwarz, B. Podmilsak, N. Mattern, and J. Eckert, J. Magn. Magn. Mater. **322**, 2298 (2010).
[9]B. L. Zink, E. Janod, K. Allen, and F. Hellman, Phys. Rev. Lett. **83**, 2266 (1999).
[10]M. B. Tang, J. Q. Wang, W. H. Wang, L. Xia, K. C. Chan, and J. T. Zhao, J. Appl. Phys. **108**, 033525 (2010).
[11]B. Zhang, D. Q. Zhao, M. X. Pan, R. J. Wang, and W. H. Wang, Acta Mater. **54**, 3025 (2006).
[12]P. Yu, R. J. Wang, D. Q. Zhao, and H. Y. Bai, Appl. Phys. Lett. **91**, 201911 (2007).
[13]F. Hellman, M. Q. Tran, A. E. Gebala, E. M. Wilcox, and R. C. Dynes, Phys. Rev. Lett. **77**, 4652 (1996).
[14]L. Xia, K. C. Chan, and M. B. Tang (unpublished).
[15]M. B. Tang, H. Y. Bai, and W. H. Wang, Phys. Rev. B **72**, 012202 (2005).
[16]R. W. Cochrane, R. Harris, J. O. Strom-Olson, and M. J. Zuckermann, Phys. Rev. Lett. **35**, 676 (1975).
[17]M. Olivier, J. O. Strom-Olsen, Z. Altounian, R. W. Cochrane, and M. Trudeau, Phys. Rev. B **33**, 2799 (1986).
[18]W. L. McMillan, Phys. Rev. B **24**, 2739 (1981).
[19]E. Abrahams, P. W. Anderson, D. C. Licciardello, and T. V. Ramakrishnan, Phys. Rev. Lett. **42**, 673 (1979).
[20]A. J. Henderson, Jr., D. G. Onn, H. Meyer, and J. P. Remeika, Phys. Rev. **185**, 1218 (1969).
[21]R. Atta-Fynn, P. Biswas, and D. A. Drabold, Phys. Rev. B **69**, 245204 (2004).
[22]M. Fukuhara, A. Kawashima, W. Zhang, A. Inoue, and F. Yin, J. Appl. Phys. **103**, 013503 (2008).
[23]M. C. Klein, F. Hache, D. Ricard, and C. Flytzanis, Phys. Rev. B **42**, 11123 (1990).